Fig. S1

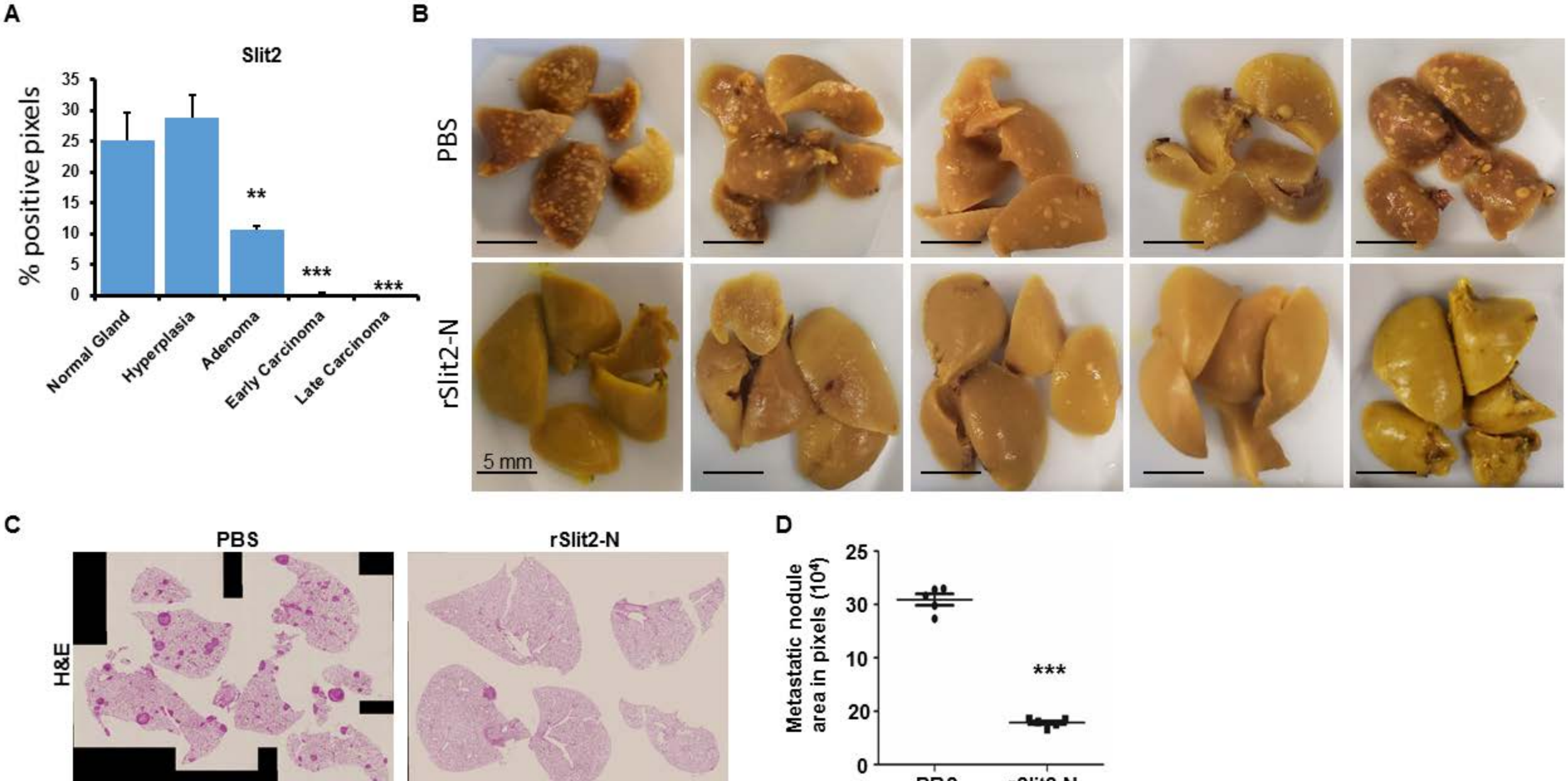
A
Slit2
% positive pixels
35
30
25
20
15
10
5
0
**
***
***
Normal Gland
Hyperplasia
Adenoma
Early Carcinoma
Late Carcinoma
B
PBS
rSlit2-N
5 mm
C
PBS
rSlit2-N
H&E
D
Metastatic nodule area in pixels (10⁴)
25
30
10
20
0
***
PBS
rSlit2-N

Fig. S1. rSlit2-N treatment inhibits lung metastases in MMTV-PyMT spontaneous mammary tumor model.

(A) Quantification of Slit2 expression in mammary glands harvested from MMTV-PyMT mice at different stages of tumor progression.

(B) Images of the lungs harvested from rSlit2 or PBS treated MMTV-PyMT mice.

C-D The lungs were processed and H&E stained. The slides were imaged under a light microscope and images were analyzed for the area of metastases using ImageJ software. **(C)** Representative H&E image of the lungs harvested from MMTV-PyMT tumors. **(D)** Quantification of metastases area in the lungs derived from (C).

** is $p<0.01$; *** is $p<0.001$ using Student's t-test.

Fig. S2

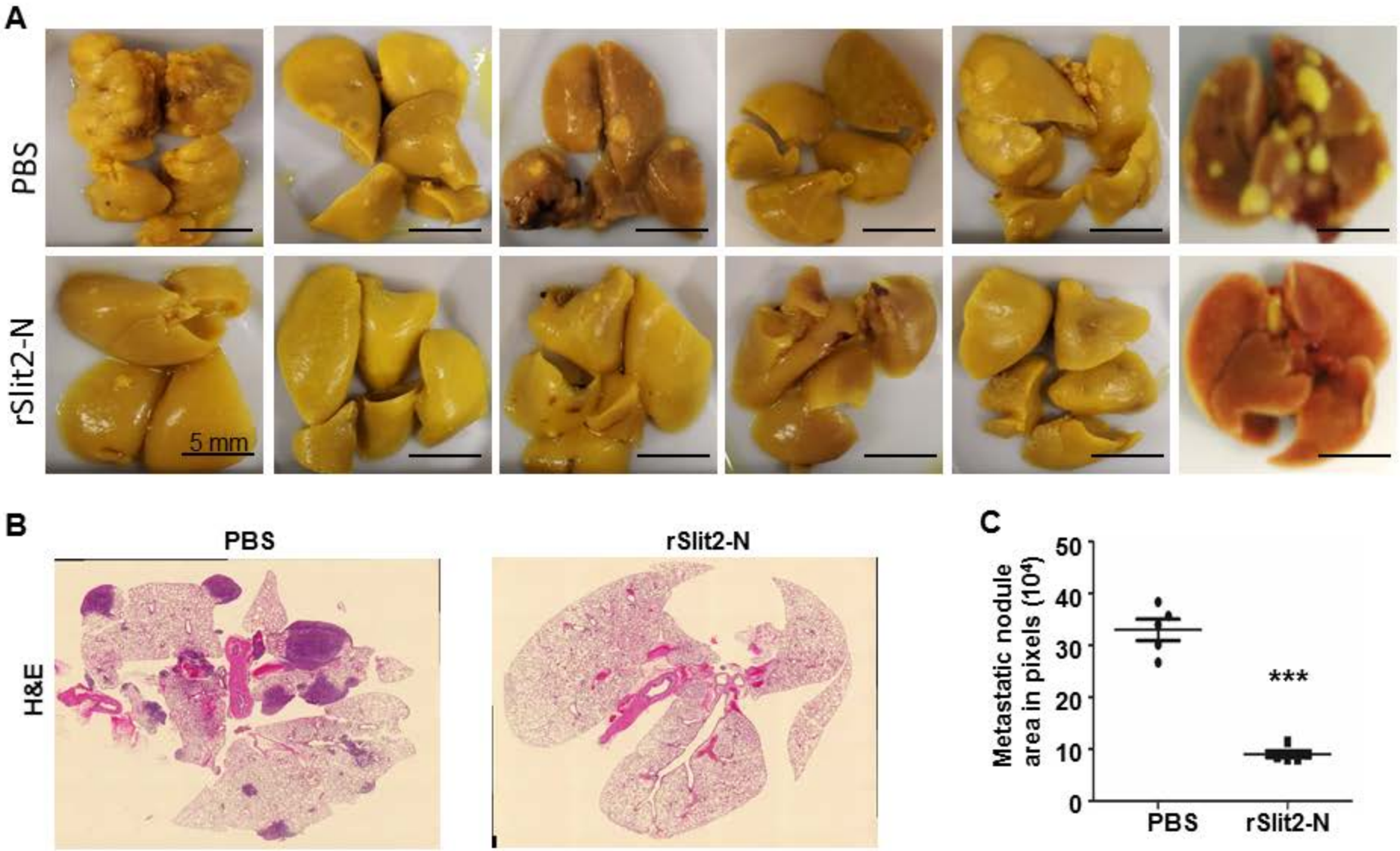
A
PBS
rSlit2-N
5 mm
B
PBS
rSlit2-N
H&E
C
Metastatic nodule area in pixels (10⁴)
50
40
30
20
10
0
***
PBS
rSlit2-N

Fig. S2. rSlit2-N treatment inhibits orthotopic syngeneic tumor metastases.

The MVT1 orthotopic syngeneic tumors bearing mice were treated with rSlit2-N or PBS. The mice were euthanized and lungs were harvested, processed, and H&E stained. The slides were imaged under a light microscope and images were analyzed for the area of metastases using ImageJ software.

(A) Images of the lungs harvested.

(B) Representative H&E image of the lungs harvested from MMTV-PyMT tumors.

(C) Quantification of metastases area in the lungs.

*** is $p<0.001$ using Student's t-test.

Fig. S3

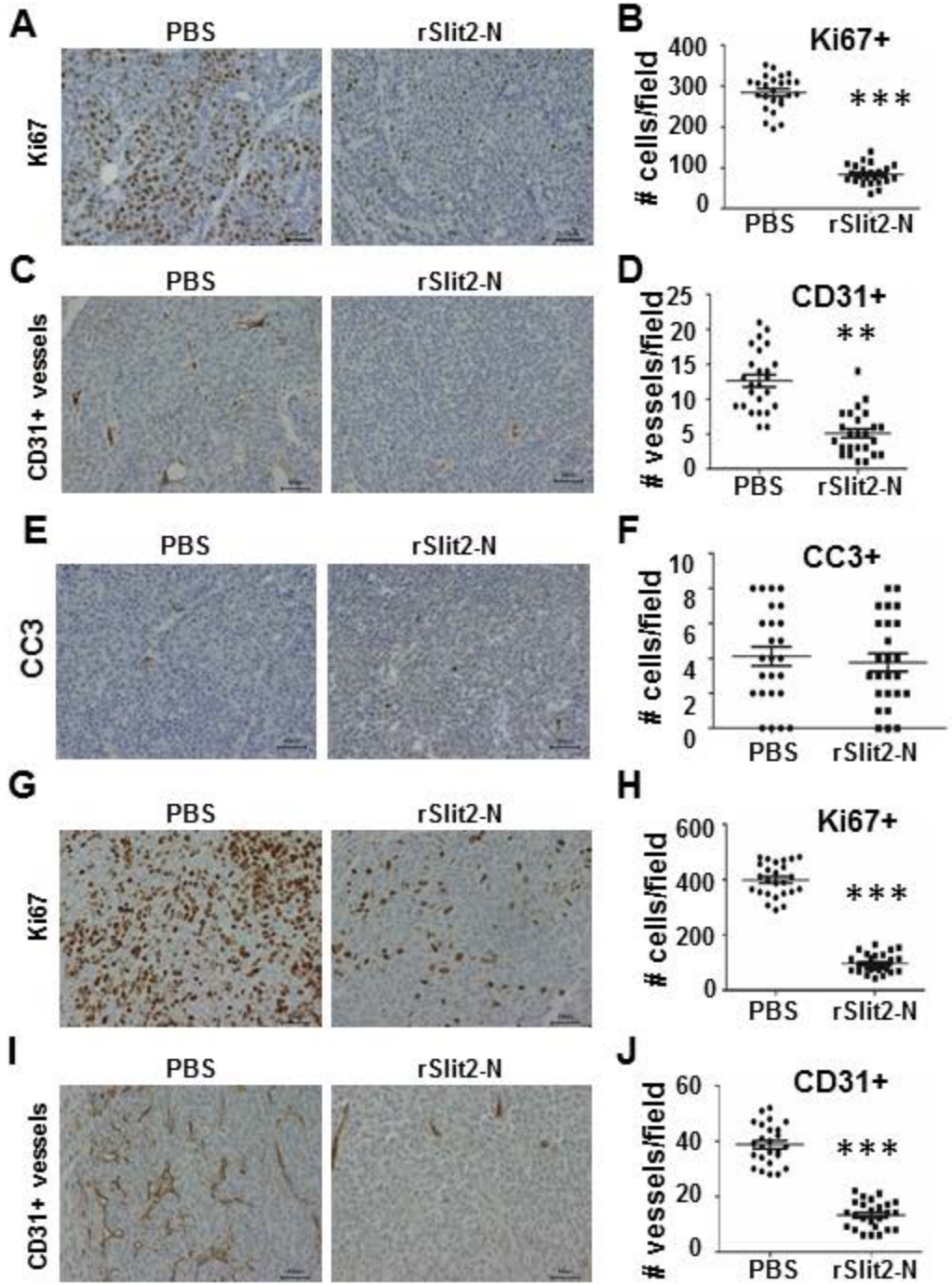
A
PBS
rSlit2-N
Ki67
B
Ki67+
cells/field
400
300
200
100
0
***
PBS
rSlit2-N
C
PBS
rSlit2-N
CD31+ vessels
D
CD31+
vessels/field
25
20
15
10
5
0
**
PBS
rSlit2-N
E
PBS
rSlit2-N
CC3
F
CC3+
cells/field
10
8
6
4
2
0
PBS
rSlit2-N
G
PBS
rSlit2-N
Ki67
H
Ki67+
cells/field
600
400
200
0
***
PBS
rSlit2-N
I
PBS
rSlit2-N
CD31+ vessels
J
CD31+
vessels/field
60
40
20
0
***
PBS
rSlit2-N

Fig. S3. Slit2 inhibits markers of tumor growth.

A-F. The tumors harvested from 12 weeks old MMTV-PyMT mice treated with rSlit2-N or PBS were processed and immunostained with different antibodies. Representative images of tumor sections immunostained with **(A)** Ki67, **(C)** CD31 antibodies, and **(E)** cleaved caspase 3 (CC3) antibody. Quantification of **(B)** Ki67+ cells per field, **(D)** the total number of CD31+ vessels, and **(F)** CC3+ apoptotic cells in the tumor sections.

G-J. The MVT1 tumors harvested from mice treated with rSlit2 or PBS were processed and immunostained with different antibodies. Representative images of tumor sections immunostained with **(G)** Ki67 and **(I)** CD31 antibodies. Quantification of **(H)** Ki67+ cells per field and **(J)** total number of CD31+ vessels per field respectively.

N= 5 each group, 5 sections from each tumor. ** is $p<0.01$; *** is $p<0.001$ using Student's t-test.

Fig. S4

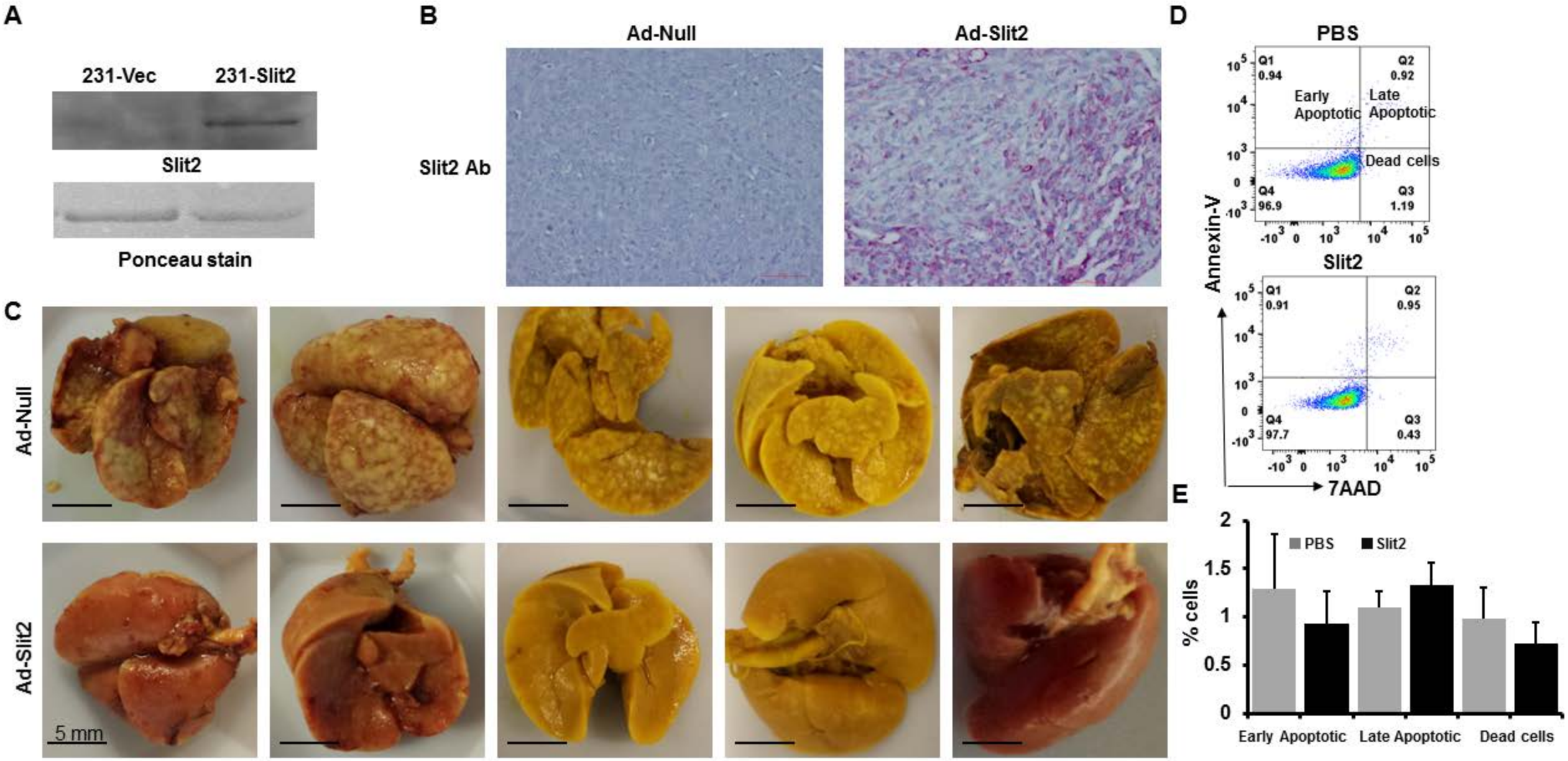
A
231-Vec
231-Slit2
Slit2
Ponceau stain
B
Ad-Null
Ad-Slit2
Slit2 Ab
C
Ad-Null
Ad-Slit2
5 mm
D
PBS
Q1 0.94
Q2 0.92
Early Apoptotic
Late Apoptotic
Dead cells
Q4 96.9
Q3 1.19
Annexin-V
Slit2
Q1 0.91
Q2 0.95
Q4 97.7
Q3 0.43
7AAD
E
PBS
Slit2
% cells
Early Apoptotic
Late Apoptotic
Dead cells

Fig. S4. Slit2 inhibits breast cancer metastases to the lungs in the xenograft mouse model.
(A) Conditioned media derived from MDA-MB-231 cells overexpressing Slit2 (231-Slit2) or vector control (231-Vec) cells were subjected to western blot analysis using anti-human Slit2 antibody. Ponceau stain was used to identify equal sample loading.

(B) The Ad-Null or Ad-Slit2 treated MDA-MB-231 xenograft tumors were immunostained with Slit2 antibody. The images showing efficient transduction of tumor tissue as evident by increased expression of Slit2 throughout the tumor, including the tumor core.

(C) Images of lungs harvested from MDA-MB-231 xenograft bearing animals treated with Ad-Null or Ad-Slit2.

D-E. MDA-MB-231 cells were treated with rSlit2-N or PBS for 24 hours and analyzed for Annexin-V positive early apoptotic or 7AAD positive dead cells or Annexin-V and 7AAD double positive late apoptotic cells by flow cytometry. (D) Flow cytometry plots showing detection of early apoptotic, late apoptotic and dead cells. (E) Quantification of apoptotic and dead cells. No statistically significant differences were observed between any of the groups.

Fig. S5

A

7 molecule(s) associated with **Osteoarthritis Pathway** at **set_1_ipa_trt-vs-ctrl - 2020-02-10 05:32 PM** [Ratio: 7/211 (0.033)] [z-score: 2.449] [p-value: 5.05E-03]

VIEW REPORT | OPEN PATHWAY

ADD TO MY PATHWAY | ADD TO MY LIST | CREATE DATASET | CUSTOMIZE TABLE | Expand

Symbol	Entrez Gene Name	Identifier	Measurement	Add/Remove column(s)	Expected	Location	Type(s)	Biomarker Applicatio...	Drug(s)
		Ensembl/Gene Symb...	Expr Log Ratio	Expr p-value					
BGLAP*	bone gamma-carboxyglut	ENSMUSG00000074483*	↑3.116	4.64E-03	↑ Up	Extracellular Space	other	diagnosis, efficacy, ...all 3	gallium nitrate ...all 1
CNMD	chondromodulin	ENSMUSG00000022025	↓-2.029	4.13E-05	↓ Down	Extracellular Space	other		
COL2A1	collagen type II alpha 1 ch	ENSMUSG00000022483	↑3.084	5.72E-06	↑ Up	Extracellular Space	other	efficacy ...all 1	collagenase clostri.....all 1
CREB3L4	cAMP responsive element	ENSMUSG00000027938	↓-4.186	1.11E-03	↓ Down	Nucleus	transcription regulator		
GDF5	growth differentiation fact	ENSMUSG00000038259	↓-2.018	5.27E-03		Extracellular Space	growth factor		
MMP10	matrix metallopeptidase 1	ENSMUSG00000047562	↑3.200	1.16E-03	↑ Up	Extracellular Space	peptidase		marimastat ...all 1
MMP13	matrix metallopeptidase 1	ENSMUSG00000050578	↑2.098	4.14E-05	↑ Up	Extracellular Space	peptidase	diagnosis ...all 1	marimastat, prino.....all 2

Selected/Total molecules: 0 / 7

B

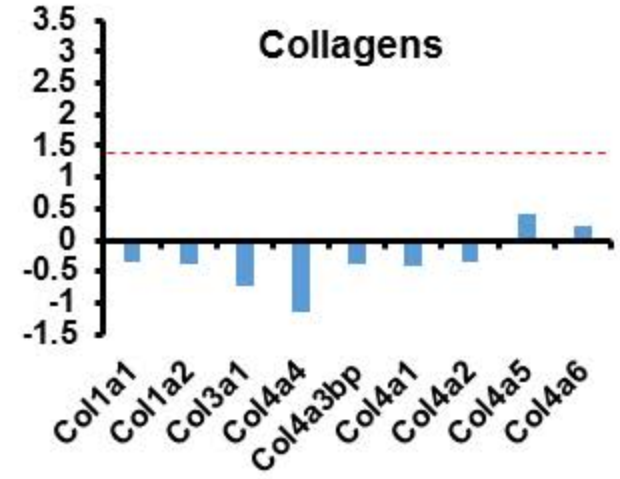

C

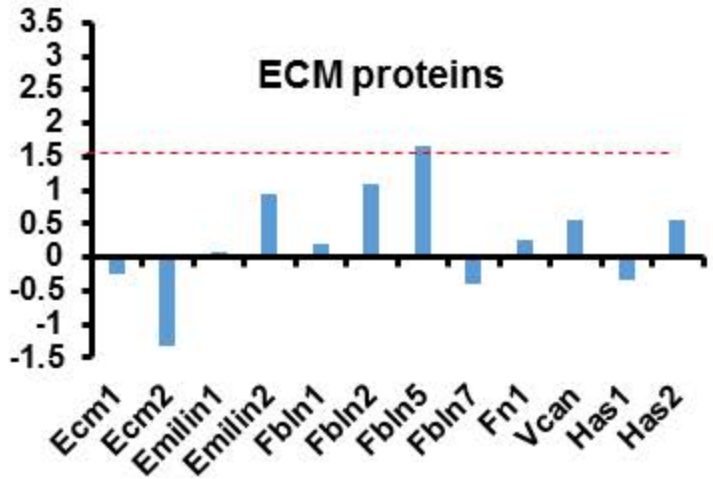

D

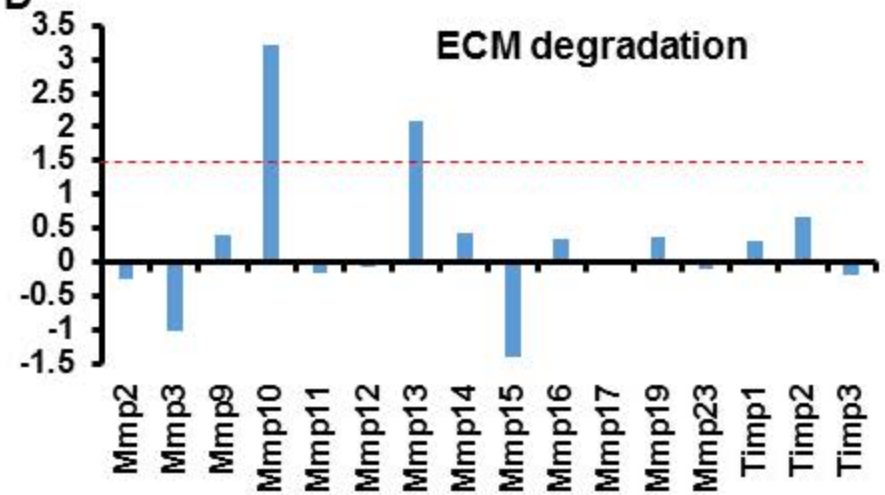

E

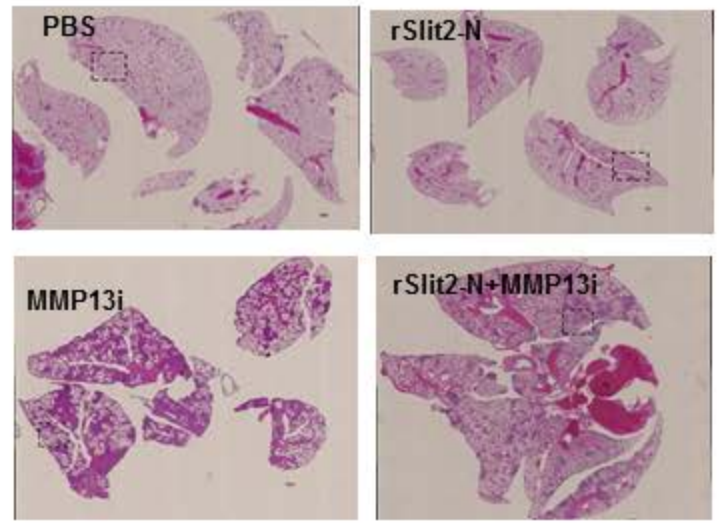

Fig. S5. rSlit2-N treatment alters the expression of ECM degradation related genes.

The tumors isolated from MMTV-PyMT mice treated with rSlit2-N or PBS were lysed and total RNA was sequenced for gene expression levels.

(A) The table shows the differentially expressed genes and statistical parameters linked to the osteoarthritis pathway identified in Fig. 1A.

B-D. Detailed analysis of ECM related genes was performed on RNASeq data from (A).

(B) Expression of different types of collagen genes.

(C) Expression of other ECM protein genes.

(D) Expression of ECM degradation related genes.

(E) Representative images of lungs harvested from MDA-MB-231 xenograft bearing animals treated with rSlit2-N or PBS in the presence or absence of MMP13 inhibitor (MMP13i).

Fig. S6

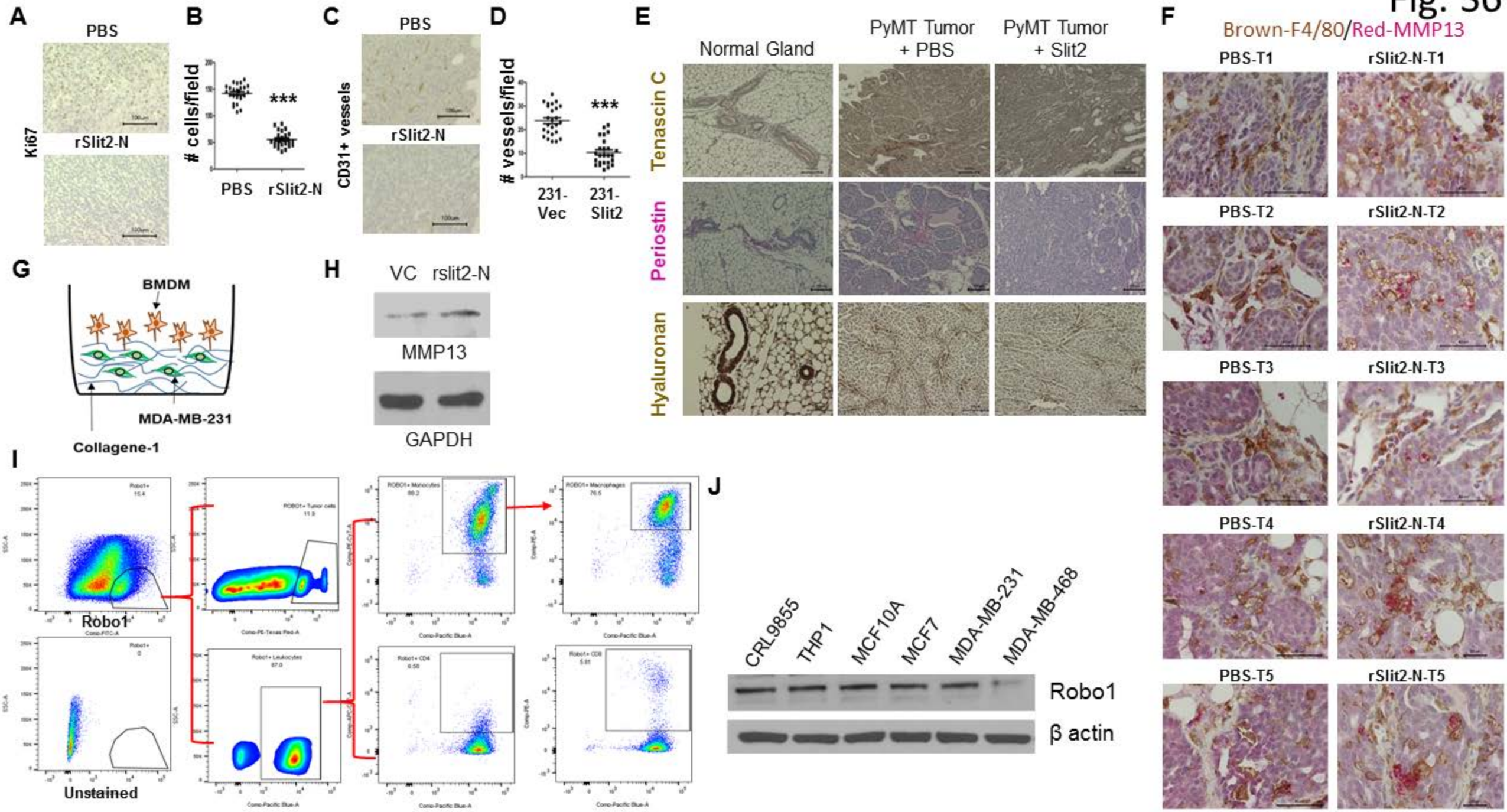
A
PBS
Ki67
rSlit2-N
B
cells/field
***
PBS
rSlit2-N
C
PBS
CD31+ vessels
rSlit2-N
D
vessels/field
***
231-Vec
231-Slit2
E
Normal Gland
PyMT Tumor + PBS
PyMT Tumor + Slit2
Tenascin C
Periostin
Hyaluronan
F
Brown-F4/80/Red-MMP13
PBS-T1
rSlit2-N-T1
PBS-T2
rSlit2-N-T2
PBS-T3
rSlit2-N-T3
PBS-T4
rSlit2-N-T4
PBS-T5
rSlit2-N-T5
G
BMDM
MDA-MB-231
Collagene-1
H
VC
rslit2-N
MMP13
GAPDH
I
Robo1
Unstained
J
CRL9855
THP1
MCF10A
MCF7
MDA-MB-231
MDA-MB-468
Robo1
β actin

Fig. S6. Analysis of TAMs-specific expression of MMP13 and Robo1 receptor.

A-D. The MDA-MB-231 xenografts treated with PBS or rSlit2-N were analyzed for proliferation and angiogenesis by IHC method. (B) Representative images showing detection of Ki67+ proliferative cells. (**C**) Quantification of Ki67+ cells detected in (B). (**D**) Representative images showing detection of CD31+ blood vessels. (**E**) Quantification of CD31+ blood vessels detected in (D). N= 5 each group, 5 sections from each tumor.

(E) The tumors harvested from 12 weeks old MMTV-PyMT mice treated with rSlit2-N or PBS or mammary glands from age matched wild type mice were processed and immunostained with different antibodies. Representative images of tumor sections immunostained with Tenascin C, Periostin, and Hyaluronan antibodies.

(**F**) The tumors harvested from PBS or rSlit2-N treated MMTV-PyMT mice were processed and sections were immunostained with F4/80 and MMP13 antibodies. The primary antibodies were detected using peroxidase-DAB and alkaline phosphatase-Red chromogen substrate systems respectively. The representative images from 5 different tumors of each group are presented here.

(G) Diagram depicting a setup for macrophage and tumor cell co-culture in the collagen matrix.

(H) BMDMs were treated with rSlit2-N or PBS. Cell lysates were analyzed for cleaved form of MMP13 expression by WB. GAPDH was used as a loading control.

(**I**)The MMTV-PyMT tumors were digested and filtered to generate the single-cell suspension. The cells were stained with Robo1 and different antibodies specific for stromal cell markers. The percentages of different types of Robo1+ cells present in the TME were identified using flow cytometry. A high percentage of Robo1-positive cells are CD45-positive lymphocytes (~87%) and about 12% of Robo1-positive cells are EpCam+ tumor cells. Further classification of Robo1+/CD45+ lymphocytes showed that 6.58% of cells are CD4-T cells, 5.81% cells are CD8-T cells and 88% cells are CD11b+ monocytes. Majority of Robo1+CD45+CD11b+ monocytes are F4/80+ macrophages (76.5%). Epcam-/CD45- stromal cells did not express Robo1.

*** is $p<0.001$ using student's t-test.

(**J)** Cell lysates from human normal breast cell line (MCF10A) and human breast cancer cell lines (MCF7, MDA-MB-231, and MDA-MB-468) and PMA-induced human THP1 and CRL9855 macrophages were analyzed for the expression of Robo1 using western blot method. β actin was used as loading control.

Fig. S7

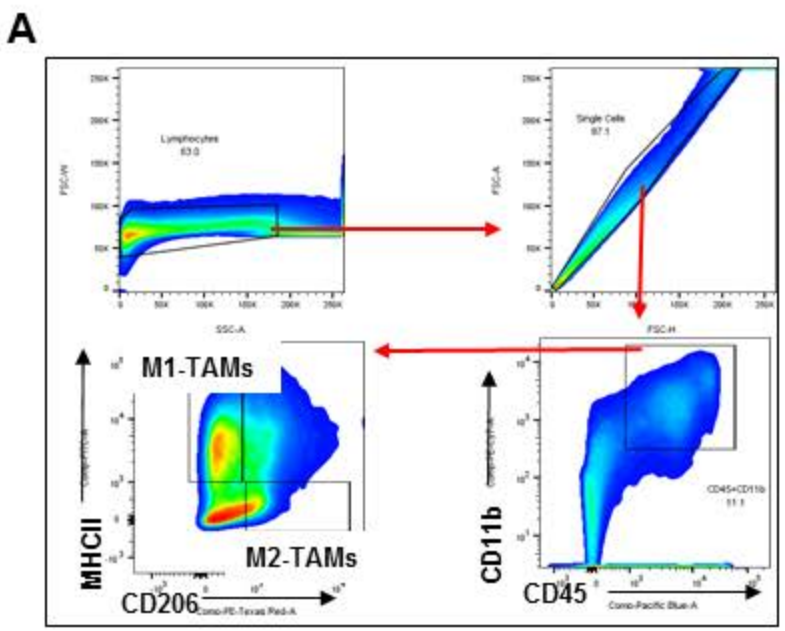
A
Lymphocytes
63.0
Single Cells
97.1
M1-TAMs
M2-TAMs
MHCII
CD206
CD11b
CD45

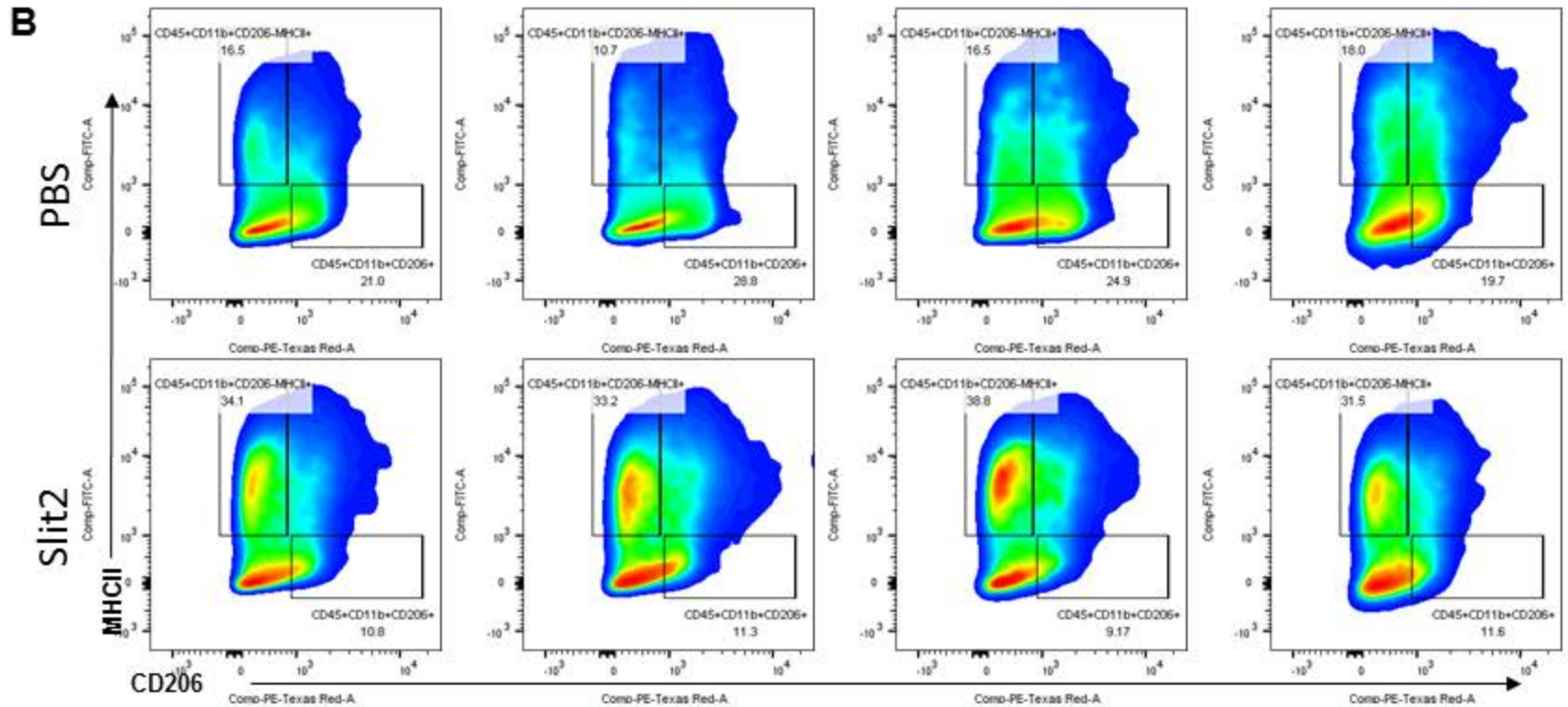
B
PBS
Slit2
CD45+CD11b+CD206-MHCII+
16.5
21.0
10.7
28.8
16.5
24.9
18.0
19.7
34.1
10.8
33.2
11.3
38.8
9.17
31.5
11.6
CD45+CD11b+CD206+
Comp-FITC-A
Comp-PE-Texas Red-A
MHCII
CD206

Fig. S7. Analysis of macrophage polarization in MMTV-PyMT tumors.

The whole tumors harvested from MMTV-PyMT mice treated with rSlit2-N or PBS were processed into single cells and flow cytometry was performed.

(A) Adopted gating strategy to identify M2-TAMs and M1-TAMs.

(B) Representative flow cytometry graphs depicting the percentage of M2-TAMs and M1-TAMs in different MMTV-PyMT tumors treated with rSlit2-N or PBS.

Fig. S8

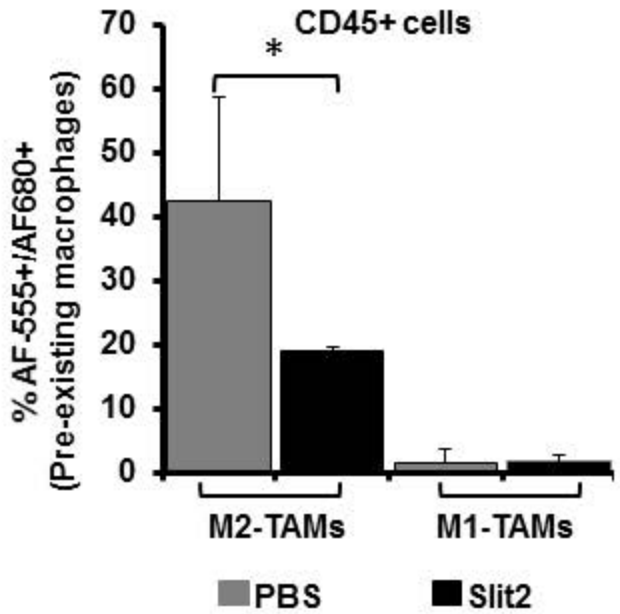
CD45+ cells
*
% AF-555+/AF680+
(Pre-existing macrophages)
70
60
50
40
30
20
10
0
M2-TAMs
M1-TAMs
PBS
Slit2

Fig. S8. rSlit2-N enhance the differentiation of tumor-derived lymphocytes into M1 type macrophages.

The flow cytometry analysis on tumor cell suspension from Fig. 3E was extended to identify M2-TAMs and M1-TAMs sub-population in pre-existing macrophages. * is $p<0.05$ using the student's t-test.

Fig. S9

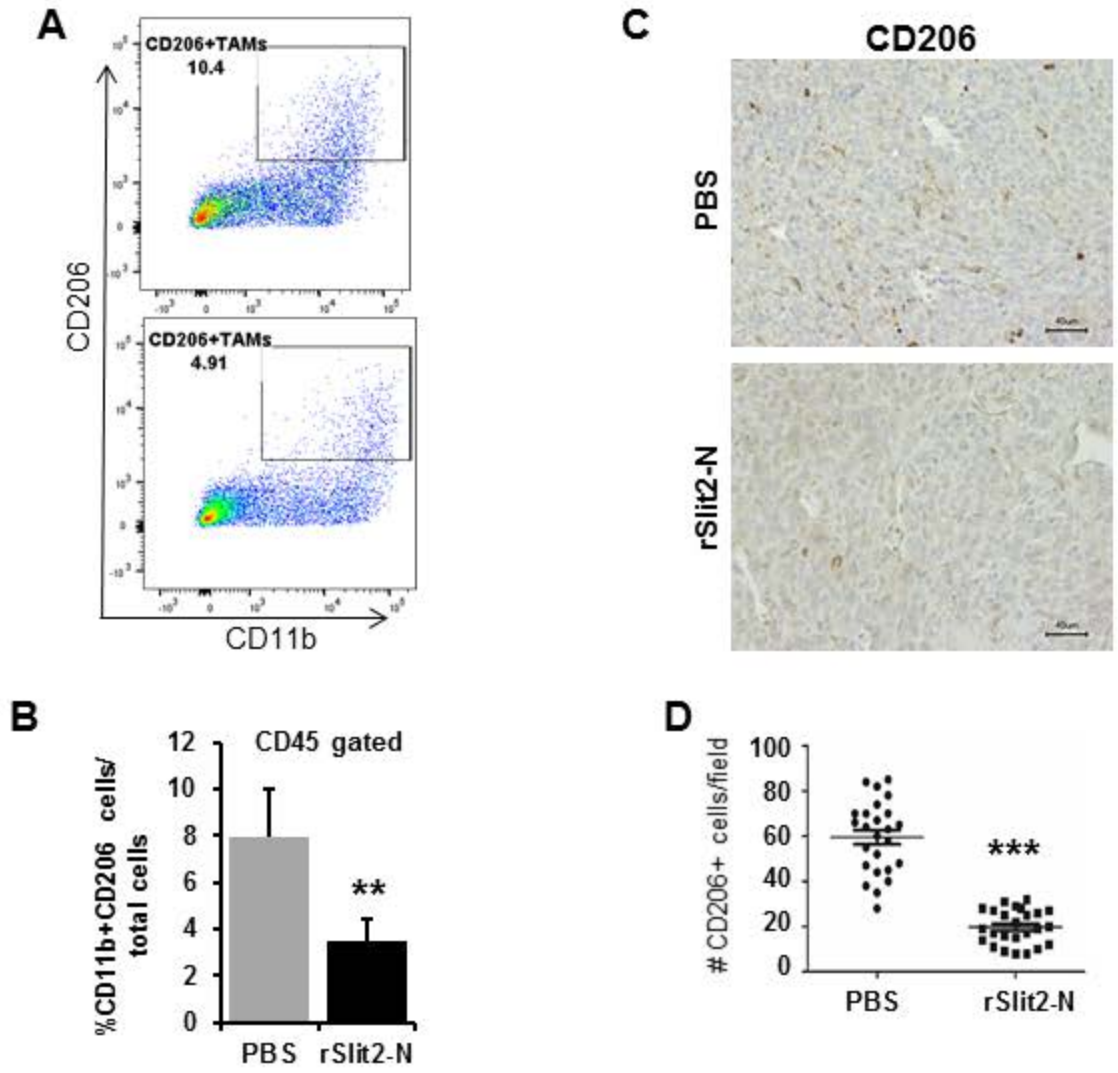
A
CD206+TAMs
10.4
CD206+TAMs
4.91
CD206
CD11b
B
CD45 gated
%CD11b+CD206 cells/ total cells
12
10
8
6
4
2
0
**
PBS
rSlit2-N
C
CD206
PBS
rSlit2-N
D
CD206+ cells/field
100
80
60
40
20
0
***
PBS
rSlit2-N

Fig. S9. rSlit2-N inhibits CD206+ TAMs in MVT1 tumors.

A-B. rSlit2-N or PBS treated MVT1 tumors were digested and filtered to the single-cell suspension. The cells were analyzed for different populations of CD206+ TAM by flow cytometry. **(A)** Representative flow cytometry graphs showing the percentage of CD206+ TAMs. **(B)** The graph depicts the quantification of CD206+ TAMs analyzed in (A). **C-D.** rSlit2-N or PBS treated MVT1 tumors were processed and sectioned to immunostained with CD206-specific antibody by IHC technique. N= 5 each group.

(C) The representative images showing CD206+ cells in the tumor sections. **(D)** The graph depicts the quantification of CD206+ cells in sections analyzed in (C). N= 5 each group, 5 sections from each tumor.

** is $p<0.01$, *** is $p<0.001$ using student's t-test.

Fig. S10

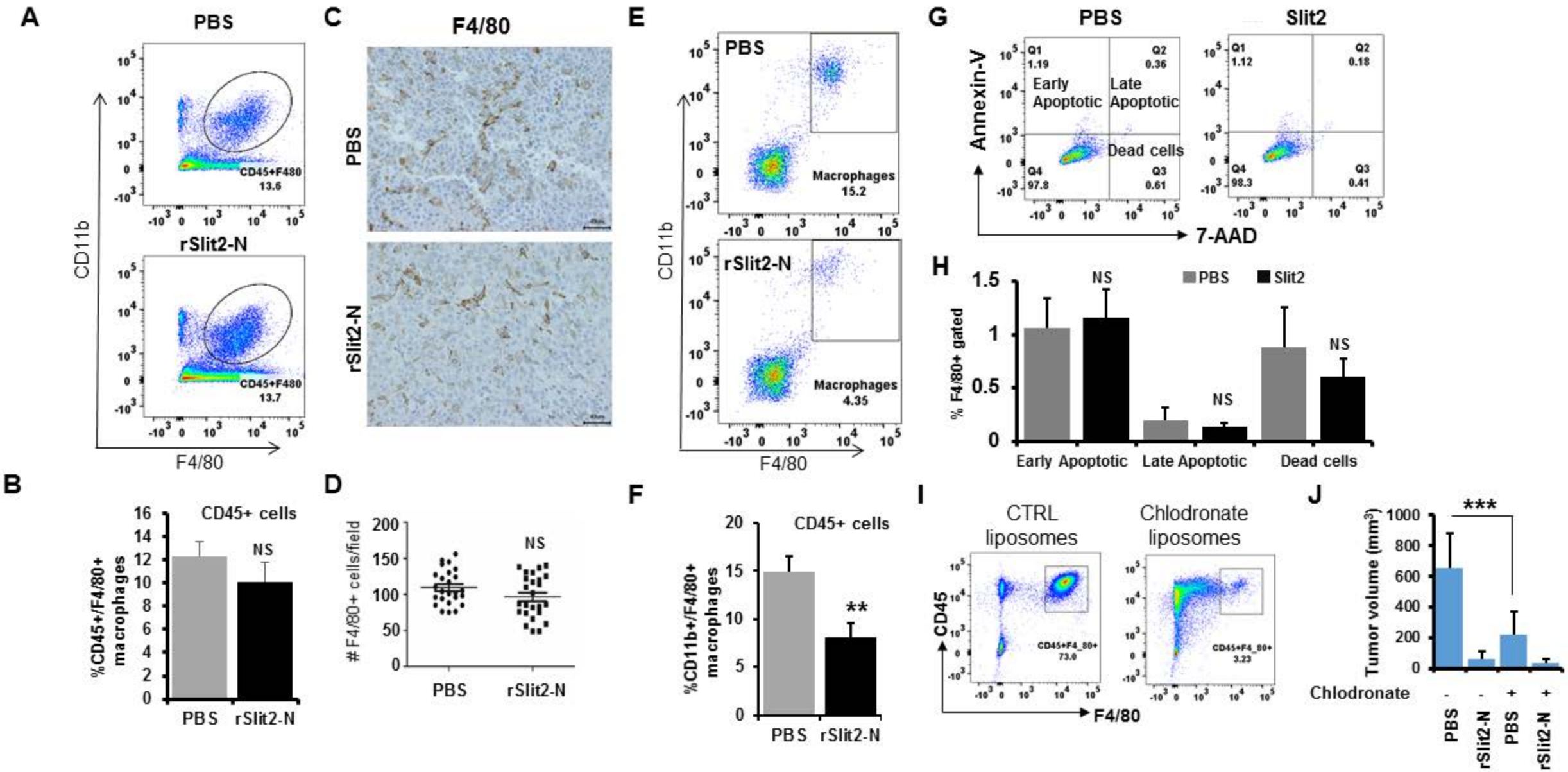
A
PBS
CD45+F480
13.6
rSlit2-N
CD45+F480
13.7
CD11b
F4/80
C
F4/80
PBS
rSlit2-N
E
PBS
Macrophages
15.2
rSlit2-N
Macrophages
4.35
CD11b
F4/80
G
PBS
Slit2
Annexin-V
Q1
1.19
Q2
0.36
Early Apoptotic
Late Apoptotic
Dead cells
Q4
97.8
Q3
0.61
Q1
1.12
Q2
0.18
Q4
98.3
Q3
0.41
7-AAD
H
PBS
Slit2
% F4/80+ gated
NS
NS
NS
Early Apoptotic
Late Apoptotic
Dead cells
B
CD45+ cells
%CD45+/F4/80+ macrophages
NS
PBS
rSlit2-N
D
F4/80+ cells/field
NS
PBS
rSlit2-N
F
CD45+ cells
%CD11b+/F4/80+ macrophages
**
PBS
rSlit2-N
I
CTRL liposomes
Chlodronate liposomes
CD45
CD45+F4_80+
73.0
CD45+F4_80+
3.23
F4/80
J
***
Tumor volume (mm3)
Chlodronate
PBS
rSlit2-N
PBS
rSlit2-N

Fig. S10. Effect of rSlit2-N on the number of macrophages recruited to the tumors and spleen.

A-B. The whole tumors harvested from MMTV-PyMT mice treated with rSlit2-N or PBS were processed into single cells and flow cytometry was performed. **(A)** Representative flow cytometry graphs showing identification of CD11b+/F4/80+ macrophages. **(B)** The quantification of macrophages was analyzed in (A). N= 5 each group.

C-D. rSlit2-N or PBS treated MMTV-PyMT tumors were processed and sectioned to immunostained with an F4/80-specific antibody to identify macrophages by the IHC technique. **(C)** The representative images showing F4/80+ cells in the tumor sections. **(D)** The graph depicts the quantification of F4/80+ cells in tissue sections analyzed in (C). N= 5 each group, 5 sections from each tumor.

E-F. The spleens harvested from MMTV-PyMT mice treated with rSlit2-N or PBS were minced and filtered into single cells and flow cytometry was performed. **(E)** The representative flow cytometry graphs showing the identification of F4/80 positive cells in the spleen samples. **(F)** The quantification of macrophages analyzed in (E). N= 5 each group.

G-H. MMTV-PyMT tumors were processed to sort F4/80+ macrophages. The sorted cells were treated with rSlit2-N or PBS for 24 hours and analyzed for Annexin-V+ early apoptotic or 7AAD+ dead cells or Annexin-V and 7AAD double positive late apoptotic cells by flow cytometry. (**G**) Flow cytometry plots showing detection of early apoptotic, late apoptotic and dead cells. (**H**) Quantification of apoptotic and dead cells. No statistically significant differences were observed between any of the groups. NS is p value not significant using student's t-test.

I-J. MDA-MB-231 xenografts bearing mice were treated with clodronate or control liposomes in the presence or absence of rSlit2-N treatment. The animals were observed for tumor growth. (**I**) The flow cytometry graphs showing efficient deletion of peritoneal macrophages in mice treated with chlodronate liposomes compared to control liposomes (CTRL). (**J**) The graph showing tumor volume at day of euthanasia.

NS is p value not significant, ** is $p<0.01$, *** is $p<0.001$ using student's t-test.

Fig. S11

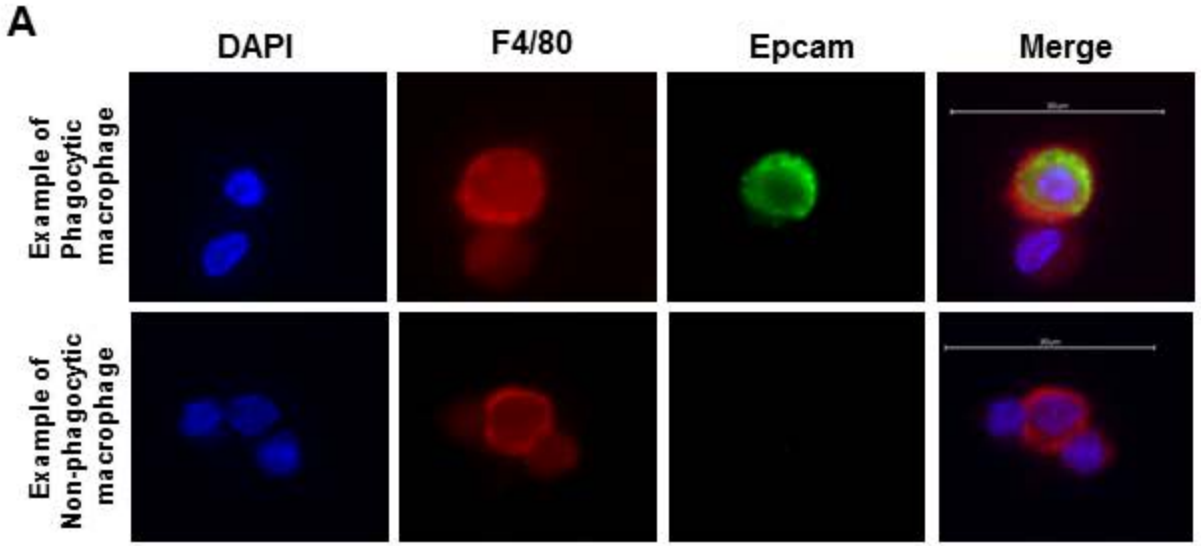
A
DAPI
F4/80
Epcam
Merge
Example of Phagocytic macrophage
Example of Non-phagocytic macrophage

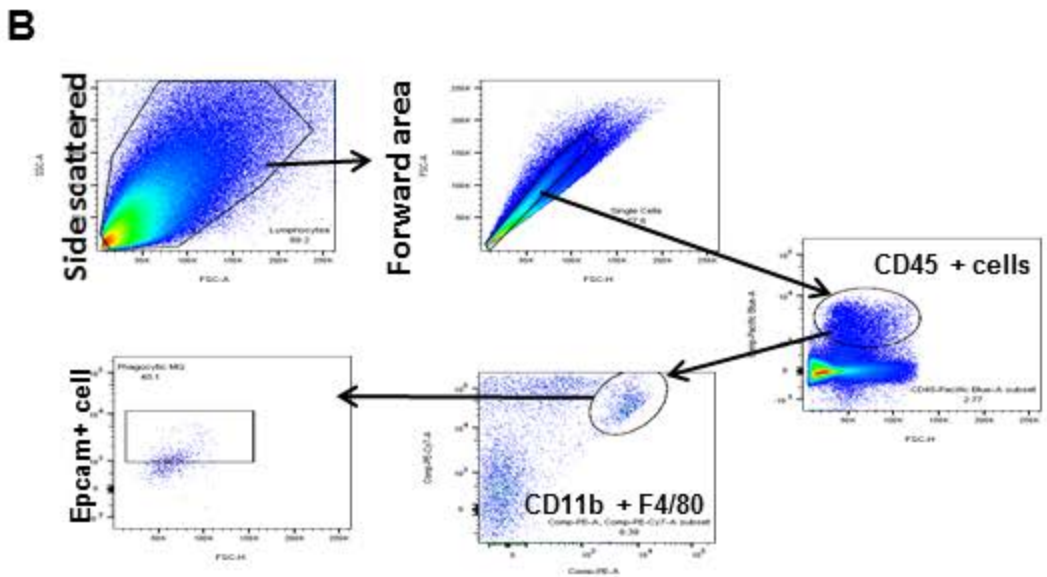
B
Side scattered
Forward area
CD45 + cells
CD11b + F4/80
Epcam+ cell

Fig. S11. Analyze the effect of rSlit2-N on the phagocytic ability of TAMs.

(A) MMTV-PyMT tumors were digested into single cells and CD11b+ cells were sorted. The cells were cytospun onto a glass slide and stained with F4/80 and Epcam antibodies. The slides were analyzed under a confocal microscope. The representative images showing an example of phagocytic and non-phagocytic macrophages.

(B) MMTV-PyMT mice were treated with rSlit2 or PBS. Whole tumors were digested into single cells and analyzed by flow cytometry. The cascade of flow cytometry graphs shows the gating strategy adopted to identify F4/80+ macrophages containing intracellular signal of tumor marker Epcam.

Fig. S12

A Brown-TAMs and Red-Cleaved caspase-3

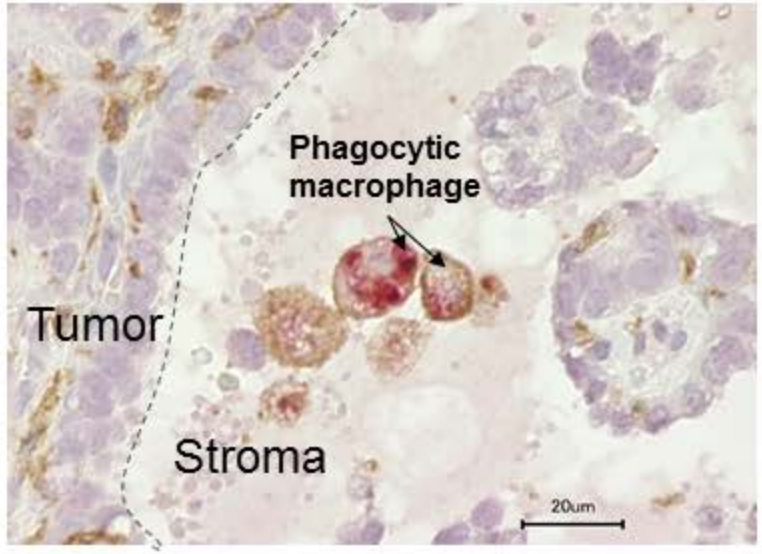

B

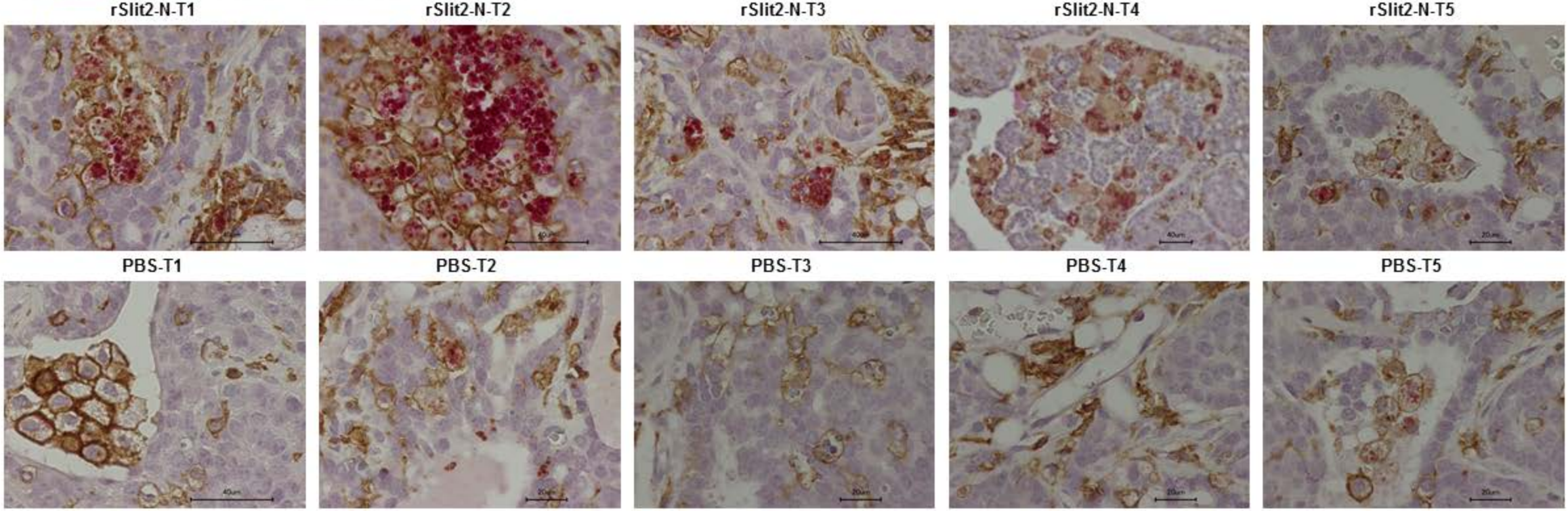

Fig. S12. Identification of phagocytic TAMs by IHC.

The tumors harvested from PBS or rSlit2-N treated MMTV-PyMT mice were processed and sections were immunostained with F4/80 and cleaved caspase 3 (CC3) antibodies. The primary antibodies were detected using peroxidase-DAB and alkaline phosphatase-Red chromogen substrate systems respectively.

(A) An example of phagocytic TAMs positive for F4/80+ and intracellular CC3.

(B) The representative images of 5 different tumors from each group.

Fig. S13

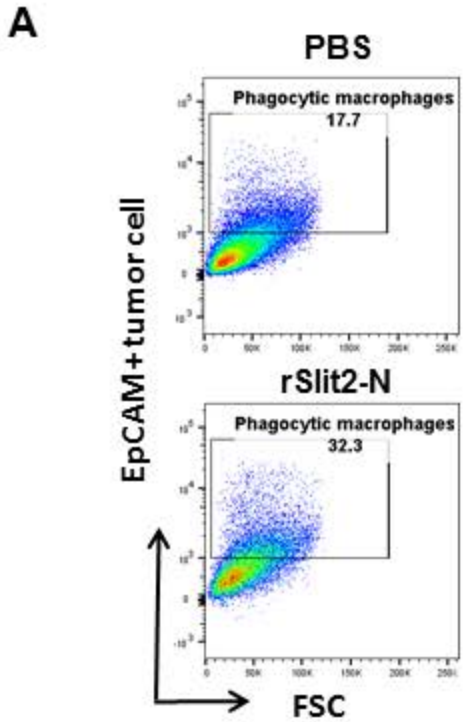
A
PBS
Phagocytic macrophages
17.7
rSlit2-N
Phagocytic macrophages
32.3
EpCAM+tumor cell
FSC

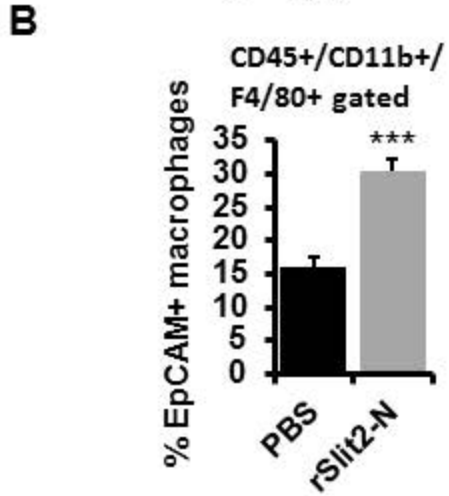
B
CD45+/CD11b+/
F4/80+ gated
% EpCAM+ macrophages
35
30
25
20
15
10
5
0
***
PBS
rSlit2-N

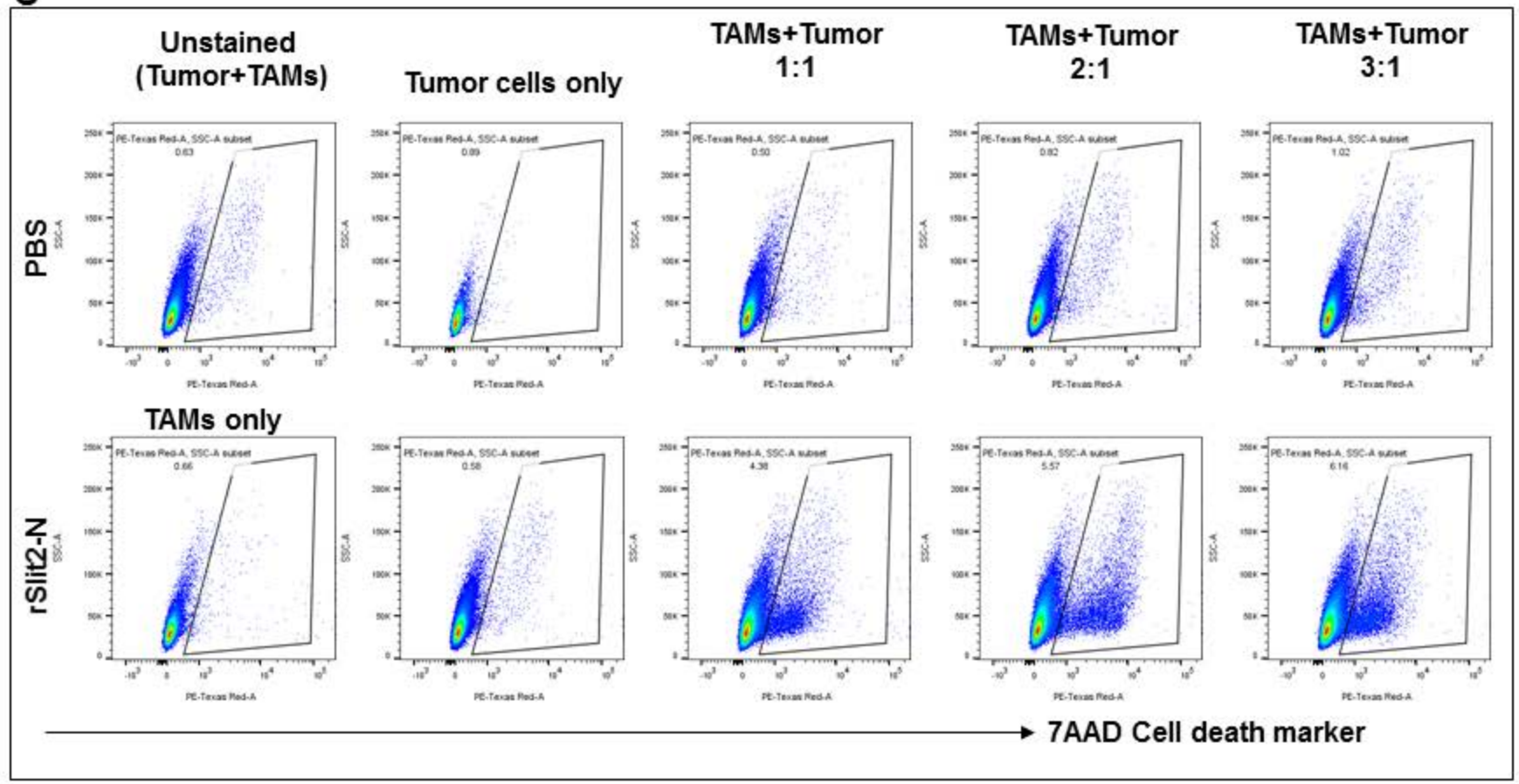
C
Unstained
(Tumor+TAMs)
Tumor cells only
TAMs+Tumor
1:1
TAMs+Tumor
2:1
TAMs+Tumor
3:1
PBS
TAMs only
rSlit2-N
7AAD Cell death marker

Fig. S13. rSlit2-N enhances the ability of TAMs to lyse tumor cells *Ex-vivo*.

A-B. Single-cell preparations from rSlit2-N or PBS treated MDA-MB-231 xenografts were analyzed for phagocytic macrophages using intracellular flow cytometry. (**A**) The cytometry plots are showing intracellular EpCAM signal inside CD45+/CD11b+/F4/80+ macrophages.

(B) The graph shows the percentage of EpCAM+ macrophages out of gated total macrophages in PBS or rSlit2-N treated tumors as identified in (A). *** is $p<0.001$ using student's t-test.

(**C**) The MMTV-PyMT tumors were processed into single cells and F4/80+ TAMs were sorted. The TAMs were pre-treated with rSlit2-N or PBS and MVT1 tumor cells were added to the TAMs. After 2 days, the cells were stained with cell death marker 7AAD and lysed cells were identified using flow cytometry.

Fig. S14

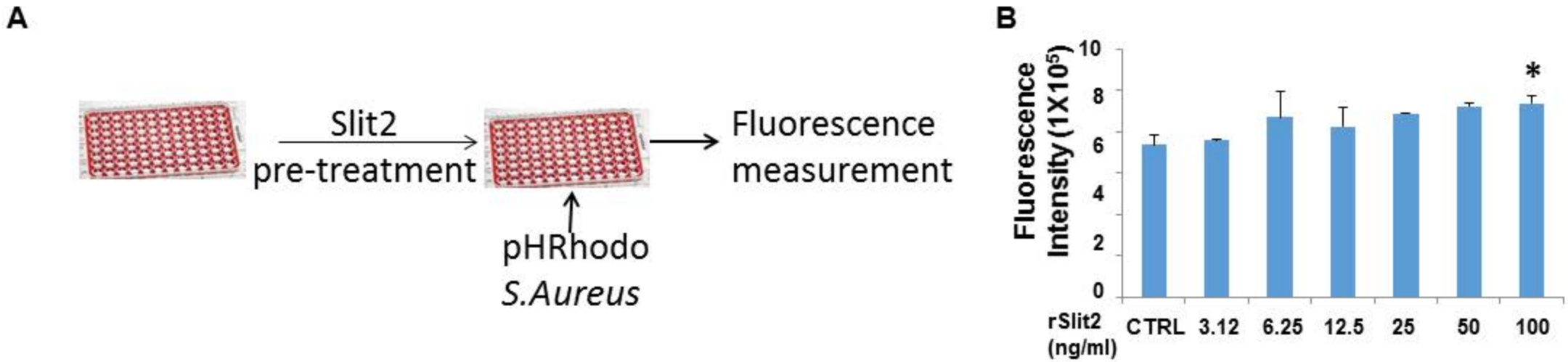
A
Slit2
pre-treatment
Fluorescence
measurement
pHRhodo
S.Aureus
B
Fluorescence Intensity (1X10^5)
10
8
6
4
2
0
*
rSlit2 (ng/ml)
CTRL
3.12
6.25
12.5
25
50
100

Fig. S14. rSlit2-N enhances the phagocytic ability of RAW264.7 macrophages.

(A) Schematic presentation of the research strategy to analyze the ability of mouse BMDMs to phagocytose pHRhodo tagged S. Aureus bacterial partials. The BMDMs were seeded to 96 wells in triplicates. The cells were pre-treated with rSlit2-N or PBS overnight, followed by the addition of pHRhodo tagged S. Aureus bacteria. The plates were incubated at 37° C in a fluorescence plate reader and kinetics of bacterial phagocytosis was analyzed for up to 4 hours.

(B) The graph represents fluorescence intensity generated by phagocytosis of bacterial particles at 3 hours and different concentrations of rSlit2-N. * is $p < 0.05$ using Student's t-test.

Fig. S15

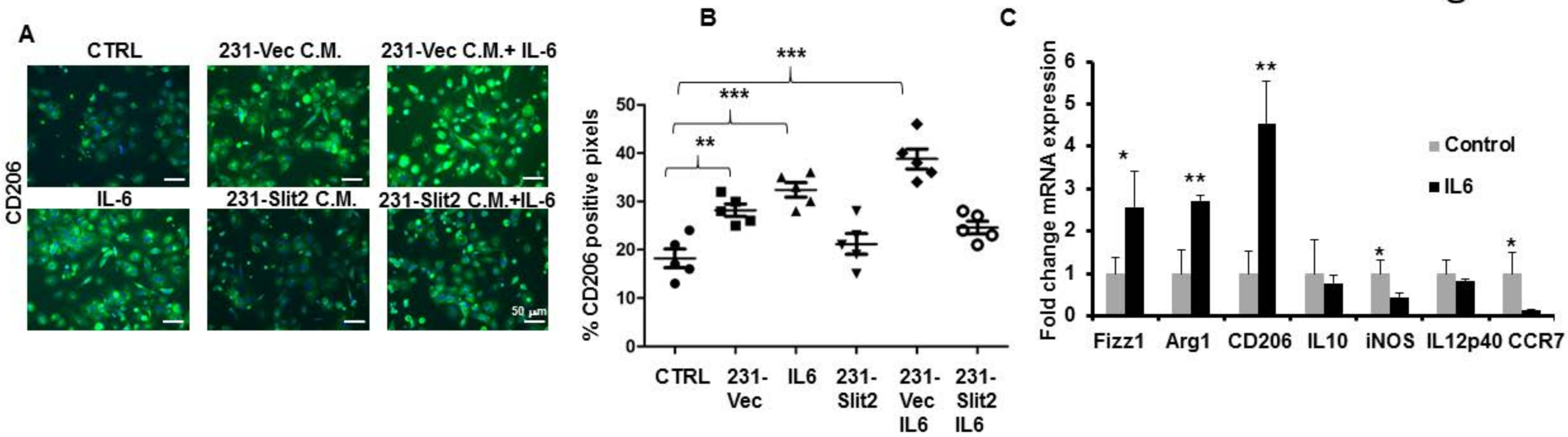
A
CTRL
231-Vec C.M.
231-Vec C.M.+ IL-6
IL-6
231-Slit2 C.M.
231-Slit2 C.M.+IL-6
CD206
50 μm
B
% CD206 positive pixels
0
10
20
30
40
50
**
***
***
CTRL
231-Vec
IL6
231-Slit2
231-Vec IL6
231-Slit2 IL6
C
Fold change mRNA expression
0
1
2
3
4
5
6
*
**
**
*
*
Control
IL6
Fizz1
Arg1
CD206
IL10
iNOS
IL12p40
CCR7

Fig. S15. IL6 induces and Slit2 inhibits M2 macrophage markers.

(A) Human monocyte cell line THP1 was induced with PMA to differentiate into macrophages. These macrophages were incubated with 231-Vec CM or 231-Slit2 CM or recombinant IL6 (10 ng/ml) for 48 hours followed by immunofluorescence staining using TAMs specific CD206 antibody. The representative images showing expression of CD206 were analyzed by a fluorescence microscope. **(B)** Quantification of CD206 expression as detected in (A).

(C) BMDMs were treated with recombinant mouse IL6 (10 ng/ml) for 48 hours. The cells were lysed and mRNA was harvested. The expression of various M1/M2 macrophage markers was analyzed by real-time PCR.

* is $p<0.05$, ** is $p<0.01$, *** is $p<0.001$ using student's t-test.

Fig. S16

A

Analysis of statistical significance for figure 6C.

Comparison	Statistical significance
Normal-vs-Luminal	<1E-12
Normal-vs-HER2Pos	<1E-12
Normal-vs-TNBC-BL1	<1E-12
Normal-vs-TNBC-BL2	3.81570330887371E-11
Normal-vs-TNBC-IM	1.62436730732907E-12
Normal-vs-TNBC-LAR	1.5701000499746E-09
Normal-vs-TNBC-MSL	9.698700E-03
Normal-vs-TNBC-M	1.62470037423645E-12
Normal-vs-TNBC-UNS	1.19209975224521E-10
Luminal-vs-HER2Pos	1.27849999476126E-08
Luminal-vs-TNBC-BL1	4.24119999997696E-06
Luminal-vs-TNBC-BL2	4.615800E-03
Luminal-vs-TNBC-IM	2.28729999995902E-06

B

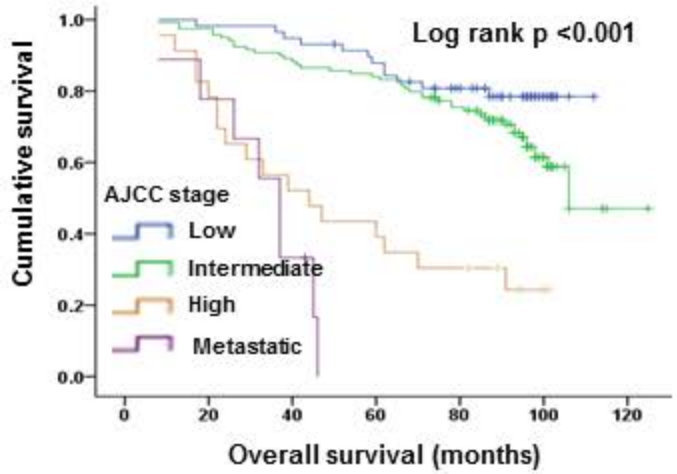

C

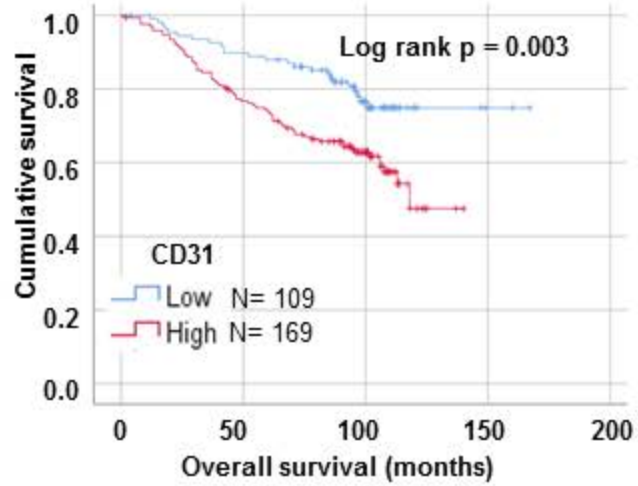

D

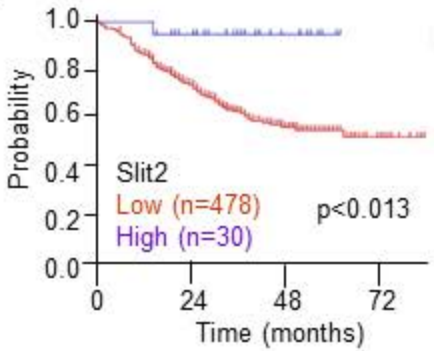

E

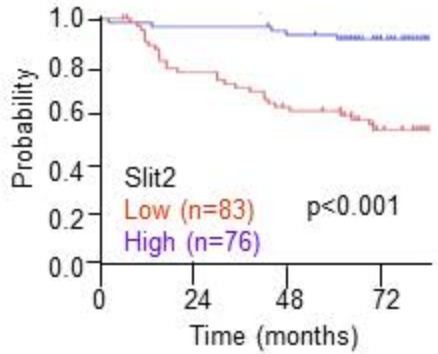

F

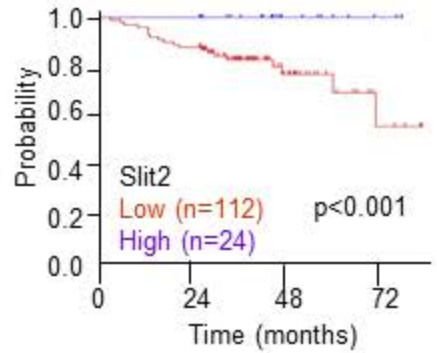

Fig. S16. Correlation of Slit2 expression levels with breast cancer patient survival.

(A) Analysis of statistical significance for Slit2 mRNA expression in human breast tissue samples presented in Fig. 6C.

B-C. Survival analysis of experimental TMA patients (n= 277) based on **(B)** tumor stage and **(C)** CD31+ blood vessels.

D-F. Slit2 expression analysis using R2 bioinformatics platform demonstrated that **(D)** high level of Slit2 correlates with better breast cancer patient survival in Booser database, n=508, **(E)** Bergh database, n=159 and **(F)** Zhang database, n=136.

Table S1. List of real time PCR primers.

Primer		Sequence (5’ – 3’)
MMP13	Forward	TGGACCTTCTGGTCTTCTGG
	Reverse	TGGGCAGCAACAATAAACAA
MMP10	Forward	CAGTTGGAGAACACGGAGAC
	Reverse	TGTCCATTTCTCATCATCATCG
MMP15	Forward	CAGGAAAGGCATGGAACAAT
	Reverse	ACCAATGGTGTGACCTGCTC
β-Actin	Forward	CAGCTTCTTTGCAGCTCCTT
	Reverse	CACGATGGAGGGGAATACAG
Arginase 1	Forward	AACACGGCAGTGGCTTTAACC
	Reverse	GGTTTTCATGTGGCGCATTC
Fizz1	Forward	ACTGCCTGTGCTTACTCGTTGACT
	Reverse	AAAGCTGGGTTCTCCACCTCTTCA
CD206	Forward	CCACAGCATTGAGGAGTTTG
	Reverse	ACAGCTCATCATTTGGCTCA
IL-10	Forward	CGGGAAGACAATAACTG
	Reverse	CATTTCCGATAAGGCTTGG
iNOS	Forward	CCAAGCCCTCACCTACTTCC
	Reverse	CTCTGAGGGCTGACACAAGG
IL-12p40	Forward	AGTATCTCTGCCTCCTTCCTT
	Reverse	GCAACACTGAAAACTAGTGTC
CCR7	Forward	AAAGCACAGCCTTCCTGTGT
	Reverse	AGTCCACCGTGGTATTCTCG
18s	Forward	GCTCTAGAATTACCACAGTTATC
	Reverse	AAATCAGTTATGGTTCCTTTGGT

Abbreviations: MMP, Matrix Metalloproteinase; CD206, Cluster of Differentiation 206; IL10, Interleukin 10; iNOS, inducible Nitric Oxide Synthase; IL12p40, Interleukin 12 p40 subunit; CCR7, C-C Chemokine Receptor 7,

Table S2. List of reagents and resources.

Reagents or resources	Source	Catalog number
Antibodies- Flow Cytometry		
Anti-mouse CD45- Brilliant Violet 421	Biolegend	103133
Anti-mouse CD11b-APC/Cy7	Biolegend	101226
Anti-mouse CD11b-PE/Cy7	Biolegend	101215
Anti- mouse F4/80-PE/Dazzle 594	Biolegend	123145
Anti- mouse F4/80-PE	Biolegend	123109
Anti- mouse MHCII-FITC	Biolegend	123107
Anti-mouse CD80-PE/Cy7	Biolegend	104733
Anti- mouse CD206-PE/Cy7	Biolegend	141719
Anti- mouse CD206-PE/ Dazzle 594	Biolegend	141731
Anti- mouse CD3 PE/Cy7	Biolegend	100219
Anti- mouse CD4-APC/Cy7	Biolegend	100413
Anti- mouse CD8-PE	Biolegend	100708
Anti- mouse Epcam- FITC	Biolegend	118207
Anti- mouse Robo1	Abcam	Ab7279
Anti-mouse CD11b-biotin	Biolegend	101204
Anti-mouse F4/80-biotin	Biolegend	123106
Anti-Biotin microbeads	Miltenyi Biotec	130-090-485
Antibody-WB, IHC and IF		
Anti-mouse Slit2	Sigma-Aldrich	SAB2701356
Anti-mouse Ki67	Invitrogen	14-5698-80
Anti-mouse CD31	Cell Signaling Technology	77699S
Anti-mouse MMP13	Novus	NBP2-17310
Anti-mouse CC3	Cell Signaling Technology	9961
Anti-mouse/human CD206	Cell Signaling Technology	91992
Anti-Mouse F4/80	AbD Serotec	MCA497G
Anti-mouse Collagen 1	Abcam	ab34710
Anti-mouse Epcam	Cell Signaling Technology	14452
Anti-mouse FAP	Abcam	Ab53066
Anti-human Slit2	ThermoFisher	PA5-31133
Anti-human CD68	Dako	M0814
Anti-human CD163	Bio-Rad	MCA1853
Anti-Human CD31	Agilent-Dako	GA61061-2
Anti-p-NF-kB	Cell Signaling	3033S
Proteins, Antibodies and Reagents		
Mouse recombinant Slit2-N	R&D Systems	5444-SL-050
Human recombinant Slit2-N	R&D Systems	8616-SL-050
Recombinant mouse Interleukin-6	PeproTech	216-16

Table S2 continued.		
Recombinant human Interleukin-6	PeproTech	200-06
Interleukin 6 neutralization antibody	BioXCell	BE0046
Goat anti-rat secondary antibody, Alexa Flour 680		A-21096
Goat anti-rabbit secondary antibody, Alexa Flour 488	Invitrogen	A32731
Goat anti-mouse secondary antibody, Alexa Flour 488	Invitrogen	A32723
Alexa-floor 555-labelled Dextran	ThermoFisher	D34679
Hyaluronic acid	Millipore Inc.	385911
Periostin	R&D Systems	MAB3548
Tenascin C	Abcam	Ab203395
Reagents or resources		
Alexa-floor 680-labelled Dextran	ThermoFisher	D34680
Fc receptor blocker	ThermoFisher	14-0161-82
Fixation/ permeabilization Diluent	Invitrogen	5223-56
permeabilization buffer	Invitrogen	0C-8333-56
Type 1 Collagen- Rat tail	BD Biosciences	354236
MACS LS column	Miltenyibiotec	130-042-401
MACS magnet	Miltenyibiotec	130-042-302
Macrophage depletion kit	Encapsula NanoSciences	CLD-8901
Trizol	Invitrogen	
VECTASHIELD® HardSet™ Antifade Mounting Medium with DAPI	Vector Laboratories	H-1500
BLOXALL Blocking Solution	Vector Laboratories	SP-6000
7AAD	BD Biosciences	559925
Phorbol-12-myristate-13-acetate (PMA)	Sigma Aldrich	16561-29-8
pH-Rhodo Green S. aureus Bioparticles	Invitrogen	P35367
Live cell imaging media	Invitrogen	A14291DJ
VectaMount mounting media	Vector Laboratories	H-5000
ProLong Gold media with DAPI	Invitrogen	P36941
MMP13 inhibitor (WAY 170523)	Tocris	2633
Commercial assays		
RNAEasy Microkit	Qiagen	74004
Cytokine Array	Ray Biotech	
ImmPRESS Goat Anti-Mouse IgG Polymer Kit, Peroxidase	Vector Laboratories	MP-7452
ImmPRESS Goat Anti-Rabbit IgG Polymer Kit, Peroxidase	Vector Laboratories	MP-7451
ImmPRESS Goat Anti-Rat IgG Polymer Kit, Alkaline Phosphatase	Vector Laboratories	MP-5404
ImmPACT DAB Substrate Kit, Peroxidase	Vector Laboratories	SK-4105

Table S2 continued.		
ImmPACT Red Substrate Kit, Alkaline Phosphatase	Vector Laboratories	SK-5105

Abbreviation: WB, Western Blot; IHC, Immunohistochemistry; IF, Immunofluorescence; CC3, Cleaved Caspase 3; MMP, Matrix Metalloproteinase; FAP, Fibroblast Activating Protein

Table S3. Differentially expressed genes in the CD11b+ TAMs sorted from rSlit2-N treated MMTV-PyMT tumors compared to PBS treatment.

Gene name	Fold change	Adj. p value
IL6	-4.68	0.00301
EMP1	-2.83	0.00301
CCL4	-3.22	0.00301
Terf2ip	-1.1	0.00531
Selp	-4.62	0.00531
Ifnb1	-4.9	0.00531
Adamts1	-2.8	0.00531
Ptx3	-2.34	0.00531
Thbd	-3.44	0.00531
Lamb3	-2.18	0.00531
Tnf	-2.81	0.00531
Gem	-4.13	0.00531
Pde4a	-2.57	0.00531
Cxcl2	-1.64	0.00531
Cxcl12	-2.92	0.00531
Col3a1	-3.82	0.00531
Irf1	-2.35	0.00531
Csf3	-3.98	0.00531
Cdkn1a	-1.3	0.00531

Table S4. The association of Slit2 expression with different prognostic markers in breast cancer tissues using breast cancer patient TMA (n=350).

		Slit2 (%)			P value
		Negative	Low	High	
Stage	1	47 (42.7)	46 (41.8)	17 (15.5)	0.624
	2	83 (48.3)	68 (39.5)	21 (12.2)	
	3	22 (46.8)	21 (44.7)	4 (8.5)	
	4	12 (63.2)	6 (31.6)	1 (5.3)	
Grade	Low	10 (35.7)	10 (35.7)	8 (28.6)	0.015
	Medium	66 (42.3)	71 (45.5)	19 (12.2)	
	High	79 (53.4)	57 (38.5)	12 (8.1)	
ER	Absent	51 (60.7)	28 (33.3)	5 (6)	0.009
	Present	114 (43)	114 (43)	38 (14)	
PR	Absent	63 (55.8)	41 (36.3)	9 (8)	0.039
	Present	99 (42.3)	101 (43.2)	34 (14.5)	
Her2	Negative	80 (48.2)	68 (41)	18 (10.8)	0.895
	Low	9 (52.9)	5 (29.4)	3 (17.6)	
	Medium	17 (51.5)	11 (33.3)	5 (15.2)	
	High	23 (52.3)	17 (38.6)	4 (9.1)	
TNBC	Yes	20 (74.1)	6 (22.2)	1 (3.7)	0.025
	No	114 (46.9)	97 (39.9)	32 (13.2)	

Abbreviation: ER, estrogen receptor; PR, progesterone receptor; Her2, human epidermal growth factor receptor 2; TNBC, triple negative breast cancer

Table 5. Correlation of Slit2 expression with various prognostic molecular markers.

			Slit2 (%)		p
		Negative	Low	High	
Trichrome	Negative	0 (0)	2 (100)	0 (0)	***
	Low	2 (5.9)	13 (38.2)	19 (55.9)	
	Medium	7 (25.9)	17 (63)	3 (11.1)	
	High	17 (44.7)	21 (55.3)	0 (0)	
CD68+ Macrophage	Negative	45 (33.8)	69 (51.9)	19 (14.3)	NS
	Low	54 (41.9)	59 (45.7)	16 (12.4)	
	High	36 (53.7)	21 (31.3)	10 (14.9)	
CD163 M2-TAMs	Negative	43 (33.9)	54 (42.5)	30 (23.6)	***
	Low	29 (33.3)	47 (54)	11 (12.7)	
	High	59 (55.1)	45 (42.1)	3 (2.8)	
CD31+ Angiogenesis	Low	32 (29.6)	57 (52.8)	19 (17.6)	*
	High	80 (46.5)	74 (43)	18 (10.5)	

Note: * is p value <0.05; *** is p value <0.001, NS is P value not significant using student's t-test.